Journal of Materials Chemistry C

Accepted Manuscript

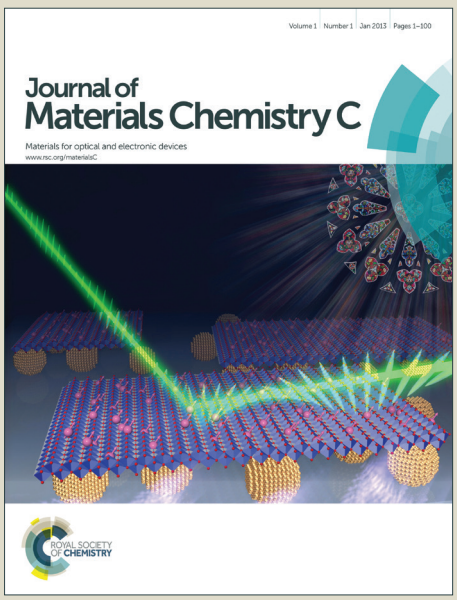

ROYAL SOCIETY OF CHEMISTRY

www.rsc.org/materialsC

Journal Name

RSCPublishing

COMMUNICATION

Properties of room-temperature ferromagnetic semiconductor in manganese doped bilayer graphene by chemical vapor deposition

Chang-Soo Park [a], Yu Zhao [b], Yoon Shon [c], Im Taek Yoon [c], Cheol Jin Lee [b], Jin Dong Song [d], Haigun Lee [e*] and Eun Kyu Kim [a*]

Cite this: DOI: 10.1039/xoxxoooooox

Received ooth January 2012,
Accepted ooth January 2012

DOI: 10.1039/xoxxoooooox

www.rsc.org/

We report the ferromagnetic graphene field effect transistor with a band gap. The Mn doped graphene has a coercive field (*Hc*) of 188 Oe and a remanent magnetization of 102 emu/cm^3 at 10 K. The temperature dependent conductivity indicates that the Mn doped graphene has a band gap of 165 meV. A fabricated graphene FET revealed the p-type semiconducting behavior, and the field effect mobility was determined to be approximately 2543 cm^{2}V^{-1}s^{-1} at room temperature.

Graphene has attracted much interest due to excellent electrical properties in the 2D monolayer with linear dispersion relation near the Dirac point, and has been broadly investigated in electronics, [1-3] solar cells,[4-6] and sensors. [7-9] The high carrier mobility at room temperature promises potential applications in nanoelectronics.[10] Furthermore, ferromagnetic semiconductors (FMS) have attracted much attention in spintronic research because future electronic devices will use a spin rather than charge in semiconductors. [11-15] Ohno et al successfully showed the properties of spin field effect transistor in InMnAs. [16] For the application of FMS, maintaining the ferromagnetic ordering at room temperature is very important. Dietl et al. had reported the possibility of room temperature ferromagnetism in semiconductors. [17] Room temperature ferromagnetism has also been reported in carbon-based materials. [18-20] Now, graphene has become hot issues for future spin electronic devices due to excellent material properties in nanoscale.[2, 3, 21, 22] However, most of ferromagnetic origins and electrical properties are far away from the function of device operation. In addition, the absence of a band gap in graphene should be resolved to utilize a graphene for application of spintronics. Therefore, it is very important to introduce the band gap to graphene and to control its transport properties for actual devices operation. The various methods have been tried to introduce a band gap in graphene. Recent studies have shown that band gap opening is possible in nanoribbons[23], bias-applied bilayer[6], strained or molecule-doped graphene [24-25], and even in substrate-induced graphene[26]. Although these methods can open up a band gap in graphene, the practical applications require a modified technology because of their difficult controllability and complexity. Among these ways to open a band gap in graphene, in-situ doping technique is very important to grow a semiconducting graphene with a band gap. In addition, to achieve manganese doping into graphene, two-layered bilayer graphene is more suitable than monolayer because the manganese atom can easily intercalate between two layers. In this study, we report the FMS properties of the manganese (Mn) doped bilayer graphene and its demonstration of field effect transistor (FET).

The Mn doped graphene film was grown by chemical vapor deposition (CVD) with two zone heaters. The 25 μm thickness of Cu film was used to grow graphene and it was inserted on the middle of CVD chamber. Additionally, manganese-dioxide powder was inserted on the second heating zone. It took 40 minutes to ramp up from room temperature to 1000 ^{o}C, and kept for 30 minutes at 1000 ^{o}C with flows of H_2 (20 sccm) and Ar (1,000 sccm). After the temperature of the second zone reached to 1000 ^{o}C for decomposition of manganese-dioxide, H_2 (20 sccm) and CH_4 (3 sccm) were supplied for 10 minutes to grow a manganese doped graphene layer on the Cu film at 1000 ^{o}C and then it took 30 minutes to cool down from 1000 ^{o}C to 50 ^{o}C by using an electric fan. The Mn doping was achieved by the carbothermal reduction, $MnO_2 + 2\ C \rightarrow Mn + 2\ CO$. The graphene grown on the Cu film placed on the Al_2O_3 plate was taken out of the CVD chamber. After growing graphene on a Cu substrate, PMMA was coated on graphene by spin coating method at 5,000 rpm for 30 sec. Cu was dissolved by Cu etchant for 30 minutes. Graphene on the PMMA film was washed in de-ionized water, and then it was transferred on a p-type doped silicon substrate coated with a 300 nm SiO_2. Thereafter, it was dried at 80 ^{o}C in an oven for 20 minutes. Pristine graphene was identified using an optical microscope. Raman spectra of the graphene films were measured for excitation of 514.5 nm at room temperature, using a Jobin-Yvon HR800UV spectrometer. Superconducting quantum interference devices (SQUID, MPMS Quantum Design)

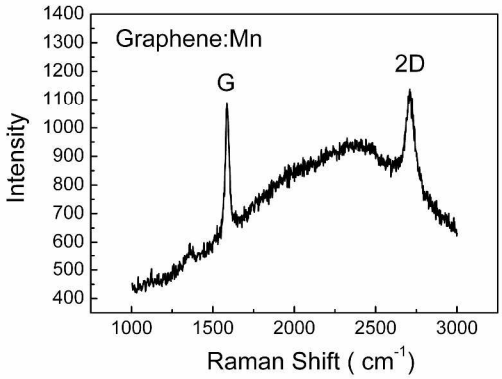

Figure 1. Raman spectra of the Mn doped bilayer graphene film on Cu substrate.

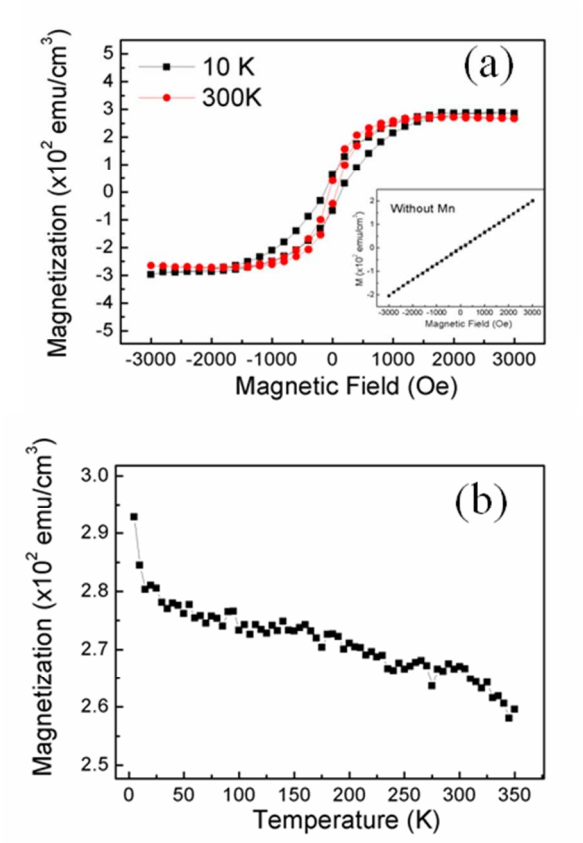

Figure 2. (a) Magnetization vs magnetic field (M-H) curves of the Mn doped graphene film at 10 K and 300 K., Inset is for undoped graphene, and (b) temperature dependent magnetization of the Mn doped graphene.

were used to characterize the magnetic properties of the graphene. The manganese composition and electronic structure were determined using X-ray photoelectron spectroscopy (XPS, ESCALAB 250 XPS spectrometer, VG Scientifics). The electrical transports were measured as a function of temperature using an I-V measurement system using Cryostat with He displex (Sumitomo).

Figure 1 shows the Raman spectra of the Mn doped bilayer graphene film on Cu after synthesis. All the areas of the sample showed the uniform Raman signal like Figure 1. Two dominant peaks clearly appeared, including the G peak at ~1569 cm^{-1}, and the 2D peak at ~2702 cm^{-1}. The peak intensity ratios (I_{2D}/I_G) of pristine graphene are approximately below unity, while the full widths at half-maximum (FWHM) of the 2D peaks are over about sixty, indicating that these samples were, in fact, bilayer graphene. [27] Figure S1 shows the fitted 2D peaks of the bilayer graphene grown by CVD. The four satellite peaks, which are $2D_{1B}$, $2D_{1A}$, $2D_{2A}$, and $2D_{2B}$ from the left, are shown as the Lorentzian fitting of the 2D peaks. Each 2D peak could be well–fit, indicating evident confirmation of bilayer graphene.

Figure 2 (a) shows magnetization curves of the Mn doped graphene taken at 10 K. It shows clear ferromagnetic hysteresis loops. The Mn doped graphene has a coercive field (*H*c) of 188 Oe and a remanent magnetization of 102 emu/cm^3 at 10 K. In particular, the Mn doped graphene has still a ferromagnetic hysteresis at room temperature, while the undoped sample without Mn has no ferromagnetic hysteresis. The measured magnetization suggests that the Mn doped graphene has large Mn particles on top of the bilayer graphene. The measured atomic percentage of Mn from XPS is 34.4%. This high ratio can be interpreted by Mn clusters on graphene, which was identified in Figure S2,3,4. The TEM plan view image shows relatively good surface including Mn although small dark dots of manganese clusters partly take place due to high Mn concentration in Figure S5 (a). The diffraction patterns contain a ring pattern due to the presence of oxidized manganese on the surface. [28] The Mn doped graphene reveals spots related to graphene and Mn. It clearly exhibits a six-fold symmetry, as expected from graphene. (Figure S5 (b)).

Recently, theoretical works have suggested that graphene may show ferromagnetism due to the existence of various defects or topological structures. [29, 30] In addition, recent results [31, 32] showed that the ferromagnetism of graphene originates from the defects in graphene. Nano-graphene edge state also showed that the edge state is electronically and magnetically active due to the presence of the non-bonding having a large local density of states with a localized spin. NEXAFS (near edge x-ray absorption fine structure) revealed the presence of the edge state located at the Fermi level and strongly spin polarization. [33, 34] However, our graphene was doped by transition metal, Mn. In addition, the weak defects peak in Raman result of Figure 1 means that the Mn doped graphene film is of very high quality. It is considered from the theoretical predictions that such a magnetism may occur if Mn atoms are trapped by single or double layer vacancies. [35] Our graphene doped with Mn is highly ferromagnetic up to above 350 K. This was shown in the temperature dependent-magnetization of the Mn doped graphene of Figure 2 (b). The Curie temperature can be estimated to be above room temperature for actual device operation. To obtain the transport properties of graphene, we have measured the temperature dependence of conductivity by conventional Hall effect system using van der Pauw method.

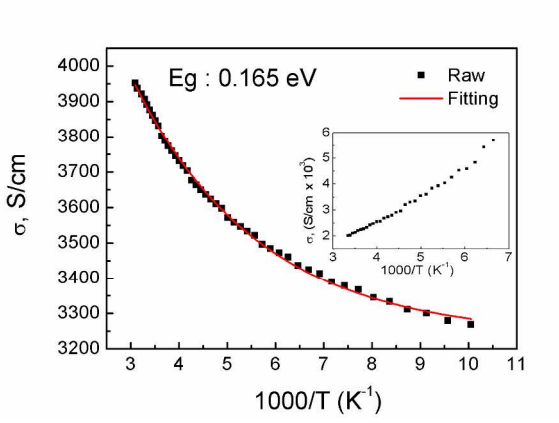

Figure 3. Temperature-dependent conductivity of the Mn doped graphene film and undoped bilayer graphene (Inset).

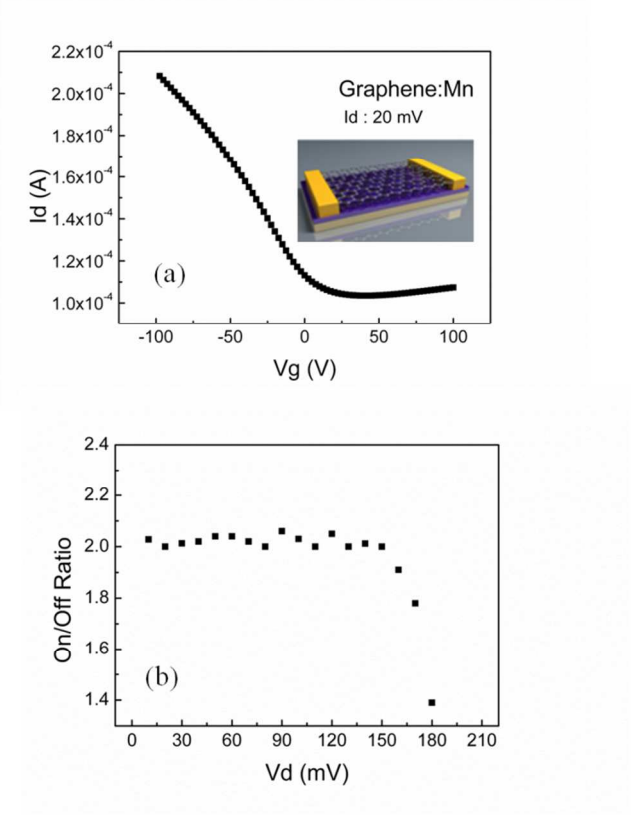

Figure 4. (a) I-V characteristics of the Mn doped graphene FET with VDS = 20 mV at room temperature. Inset is a schematic of back-gate bilayer graphene FET. (b) The Ion/Ioff ratio according to the source-drain voltage (VDS) for the Mn doped graphene FET.

Figure 3 shows the conductivity versus temperature of the Mn doped graphene. The temperature-dependent conductivity was measured in the temperature range from 150 to 300 K. The conductivity of the Mn doped graphene increases with increasing temperature like a usual semiconductor, and then can be fitted by the conductivity equation. According to the previous work, the temperature-dependent conductivity of graphene at very low temperatures can be well explained by the variable range hopping (VRH) mechanism. But thermally activated (TA) conduction is the main transport mechanism at high temperature, over 100K. The TA model can be described as: $\sigma = \sigma_0 \exp(-E_g/2kT)$ for high temperature regions over 100 K.[36] The observed band gap energy of the Mn doped graphene is determined to be 165 meV as shown in Figure 3. However, the undoped graphene as shown in inset of Figure 3 showed usual metallic properties with no band gap.

We fabricated back-gate FETs using the Mn doped bilayer graphene. The inset in Fig. 4 (a) shows a three-dimensional schematic of a back-gate bilayer graphene FET. The bilayer graphene was formed after transfer onto a 300-nm-thick SiO2/Si substrate and used as a channel. A 50-nm gold layer deposited by e-beam evaporation was used as source and drain electrodes. The channel length was 10 μm, and the channel width was 100 μm. Figure 4 (a) shows I-V characteristics of the graphene FET device with V_{DS} = 20 mV at room temperature. Here, the I-V curve from the graphene FET clearly indicates a semiconductor behavior with p-type. The field effect mobility of holes and electrons was determined by estimating the linear region of I-V curves using the equation, $\mu = (L/WC_{ox}V_d)(\Delta I_d/\Delta V_g)$; where, L and W are the channel length and width, respectively, and C_{ox} is the gate capacitance for the 300-nm-thick SiO_2. Then, the source-drain voltage (V_{DS}) was fixed at 20 mV. The field effect mobility was calculated to be 2543 $cm^2V^{-1}s^{-1}$ for the Mn doped graphene. The previous reports announced that the band gap of graphene can be estimated from the maintenance of I_{on}/I_{off} ratio relative to voltage of source-drain.[37] Thus, in order to obtain a band gap of graphene, we investigated the I_{on}/I_{off} ratio according to the voltage between the source electrode and the drain electrode (V_{DS}). Figure 4 (b) shows that the I_{on}/I_{off} ratio is about 2.1 and is maintained before V_{DS} up to 165 mV, whereas this ratio decreases drastically when the V_{DS} is higher than this value, which suggests that the band gap is about 165 meV. This value is well consistent with the result of temperature dependence of the conductivity of Figure 3.

Conclusions

In conclusion, we demonstrated the ferromagnetic graphene field effect transistor with a band gap by two-zone CVD. The Mn doped graphene has a coercive field (*Hc*) of 188 Oe and a remanent magnetization of 102 emu/cm^3 at 10 K. The temperature dependent conductivity indicates that the Mn doped graphene has a band gap of 165 meV. This result suggests that tuning of the energy band gap is possible by doping of manganese. A fabricated back-gate graphene FET revealed the p-type semiconducting behavior, and the field effect mobility was determined to be approximately 2543 $cm^2V^{-1}s^{-1}$ at the band gap energy of 165 meV. These results suggest a boosting of the spintronics application for future graphene electronics.

This work was supported in part by the National Research Foundation of Korea (NRF) grant funded by the Korea government (MSIP)(NRF-2013R1A2A2A01015824, NRF-2014R1A2A2A01007718). We also acknowledge the financial support from the Basic Science Research Program (NRF-2013R1A1A2008875, NRF-2014R1A2A2A01007718) through the

National Research Foundation of Korea, funded by the Ministry of Education. This work also was supported by the Mid-Career Researcher Program through a National Research Foundation grant funded by the Ministry of Science and Technology (2012-046999).

Notes and references

[a]Department of Physics and Quantum-Function Research Laboratory, Hanyang University, Seoul 133-791, Korea Email: ek-kim@hanyang.ac.kr Tel: +82 2 2220 0914

[b]School of Electrical Engineering, Korea University, Seoul 136-701, Republic of Korea

[c]Quantum Functional Semiconductor Research Center, Dongguk University, Seoul 100-715, Republic of Korea

[d]Center for Spintronics Research, Korea Institute of Science and Technology, Seoul 136-791, Republic of Korea

[e]Department of Materials Science Engineering, Korea University, Seoul 136-701, Republic of Korea Email: haigunlee@korea.ac.kr Tel: +82 2 3290 3265

Electronic Supplementary Information (ESI) available: [S1, Lorentzian fitting of 2D peaks of graphene; S2, optical microscope images of graphene; S3, wide scan of XPS; S4, C 1s and Mn 2p peaks of graphene. S5, TEM results]. See DOI: 10.1039/c000000x/

1 K. S. Novoselov, A. K. Geim, S. V. Morozov, D. Jiang, Y. Zhang, S. V. Dubonos, I. V. Grigorieva, and A. A. Firsov, *Science* 2004, **306**, 666.
2 K. S. Novoselov, A. K. Geim, S. V. Morozov, D. Jiang, M. I. Katsnelson, I. V. Grigorieva, S. V. Dubonos, and A. A. Firsov, *Nature* 2005, **438**, 197.
3 Y. Zhang, Y.-W. Tan, H. L. Stormer, and P. Kim, *Nature* 2005, **438**, 201.
4 Z. Liu, Q. Liu, Y. Huang, Y. Ma, S. Yin, X. Zhang, W. Sun, and Y. Chen, *Adv. Mater.* 2008, **20**, 3924.
5 Y.-B. Tang, C. S. Lee, J. Xu, Z. T. Liu, Z. H. Chen, Z. He, Y. L. Cao, G. Yuan, H. Song, L. Chen, L. Luo, H. M. Cheng, W. J. Zhang, I. Bello and S. T. Lee, *ACS Nano* 2010, **4**, 3482.
6 Y. Zhang, T.-T. Tang, C. Girit, Z. Hao, M. C. Martin, A. Zettl, M. F. Crommie, Y. R. Shen, and F. Wang, *Nature* 2009, **459**, 820.
7 F. Schedin, A. K. Geim, S. V. Morozov, E. W. Hill, P. Blake, M. I. Katsnelson, and K. S. Novoselov, *Nat Mater* 2007, **6**, 652.
8 H. G. Sudibya, Q. He, H. Zhang, and P. Chen, *ACS Nano* 2011, **5**, 1990.
9 L. A. L. Tang, J. Wang, and K. P. Loh, *J. Ame. Chem. Soc.* 2010, **132**, 10976.
10 K. S. Novoselov, Z. Jiang, Y. Zhang, S. V. Morozov, H. L. Stormer, U. Zeitler, J. C. Maan, G. S. Boebinger, P. Kim and A. K. Geim, *Science* 2007, **315**, 1379.
11 G. A. Prinz, *Science* 1998, **282**, 1660.
12 H. Ohno, *Science* 1998, **281**, 951.
13 H. Ohno, A. Shen, F. Matsukura, A. Oiwa, A. Endo, S. Katsumoto, and Y. Iye, *Appl. Phys. Lett.* 1996, **69**, 363.
14 Y. Shon, Y. H. Kwon, S. U. Yuldashev, J. H. Leem, C. S. Park, D. J. Fu, H. J. Kim, T. W. Kang, and X. J. Fan, *Appl. Phys. Lett.* 2002, **81**, 1845.
15 Y. Shon, et al., *Appl. Phys. Lett*. 201, **99**, 192109.
16 H. Ohno, D. Chiba, F. Matsukura, T. Omiya, E. Abe, T. Dietl, Y.Ohno, and K. Ohtani, *Nature* 2000, **408**, 944.
17 T. Dietl, H. Ohno, F. Matsukura, J. Cibert, and D. Ferrand, *Science* 2000, **287**, 1019.
18 P. Esquinazi, D. Spemann, R. Hohne, A. Setzer, K. H. Han, and T. Butz, *Phys. Rev. Lett.* 2003, **91**, 227201.
19 C. S. Park, X. Z. Jin, K. N. Yun, Y. R. Park, Y. Shon, N.-K. Min, and C. J. Lee, *Appl. Phys. Lett.* 2012, **100**, 192409.
20 C. S. Park,Y. Zhao, H. Kim, Y. Shon, E. K. Kim, *Chem Comm,* 2014, **50**, 12930.
21 M. B. Lundeberg and J. A. Folk, *Nat Phys* 2009, **5**, 894.
22 I. Calizo, W. Bao, F. Miao, C. N. Lau, and A. A. Balandin, *Appl. Phys. Lett.* 2007, **91**, 201904.
23 M. Y. Han, B. Ozyilmaz, Y. Zhang, and P. Kim, *Phys. Rev. Lett.* 2007, **98**, 206805.
24 F. Guinea, M. I. Katsnelson, and A. K. Geim, *Nat Phys* 2010, **6**, 30.
25 T. Ohta, A. Bostwick, T. Seyller, K. Horn, and E. Rotenberg, *Science* 2006, **313**, 951.
26 J.-K. Lee, S. Yamazaki, H. Yun, J. Park, G. P. Kennedy, G. T. Kim, O. Pietzsch, R. Wiesendanger, S. W. Lee, S. Hong, U. Dettlaff-Weglikowska, and S. Roth, *Nano Letters* 2013, **13**, 3494.
27 A. C. Ferrari, J. C. Meyer, V. Scardaci, C. Casiraghi, M. Lazzeri, F. Mauri, S. Piscanec, K. S. Novoselov, S. Roth, and A. K. Geim, *Phys. Rev. Lett.* 2006, **97**, 187401.
28 Y. Shon, S. Lee, D. Y. Kim, T. W. Kang, Chong S. Yoon, E. K. Kim and J. J. Lee, *New J. Phys.* 2008. **10**, 115002.
29 K. Harigaya, *J. Phys.: Conden. Matter* 2001, **13**, 1295.
30 H. Lee, Y.-W. Son, N. Park, S. Han, and J. Yu, *Phys. Rev. B* 2005, **72**, 174431.
31 Y. Wang, Y. Huang, Y. Song, X. Zhang, Y. Ma, J. Liang, and Y. Chen, *Nano Letters* 2008, **9**, 220.
32 L. Pisani, B. Montanari and N. M. Harrison, *New J. Phys.* 2008, **10**, 033002.
33 S.-J. Hao, V. L. J. Joly, S. Kaneko, J.-I. Takashiro, K. Takai, H. Hayashi, T. Enoki, and M. Kiguchi, *Phys. Chem. Chem. Phys.* 2014, **16**, 6273.
34 E. Velez-Fort, M. G. Silly, R. Belkhou, A. Shukla, F. Sirotti, and A. Ouerghi, *Appl. Phys. Lett.* 2013, **103** 83101.
35 A.V. Krasheninnikov, P.O. Lehtinen, A.S. Foster, P. Pyykkö, R.M. Nieminen, Phys. Rev. Lett., 2009, **102,** 126807.
36 H. Miyazaki, K. Tsukagoshi, A. Kanda, M. Otani, and S. Okada, *Nano Letters* 2010, **10**, 3888.
37 Y.-B. Tang, L. C. Yin, Y. Yang, X. H. Bo, Y. L. Cao, H. E. Wang, W. J. Zhang, I. Bello, S. T. Lee, H. M. Cheng, and C. S. Lee, *ACS Nano* 2012, **6**, 1970.

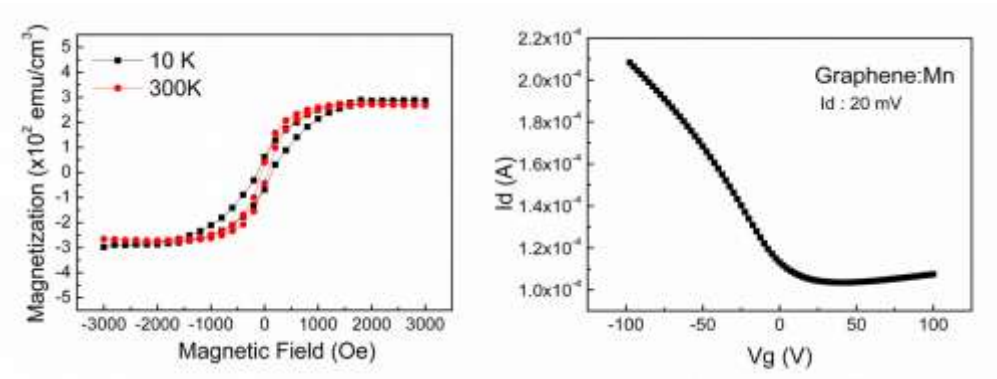

Graphical Abstract
340x128mm (96 x 96 DPI)